Multiomics characterization of low-grade serous ovarian carcinoma identifies potential biomarkers of MEK-inhibitor sensitivity and therapeutic vulnerability

Raunak Shrestha[1,2,3,*], Marta Llaurado Fernandez[4,*], Amy Dawson[4], Joshua Hoenisch[4], Stanislav Volik[1], Yen-Yi Lin[1,2], Shawn Anderson[1], Hannah Kim[4], Anne M. Haegert[1], Shane Colborne[5], Nelson K. Y. Wong[4,6], Brian McConeghy[1], Robert H. Bell[1], Sonal Brahmbhatt[1], Cheng-Han Lee[6], Gabriel E. DiMattia[7], Stephane Le Bihan[1], Greg B. Morin[5,8], Colin C. Collins[1,2,†], and Mark S. Carey[4,†]

[1]Vancouver Prostate Centre, 2660 Oak St, Vancouver, BC V6H 3Z6, Canada.

[2]Department of Urologic Sciences, University of British Columbia, 2775 Laurel Street, Vancouver, BC V5Z 1M9, Canada.

[3]Department of Radiation Oncology, University of California San Francisco, 1825 4th St., San Francisco, CA 94158, USA.

[4]Division of Gynecologic Oncology, Department of Obstetrics and Gynecology, University of British Columbia, 2775 Laurel Street, 6th Floor DHCC, Vancouver, BC V5Z 1M9, Canada.

[5]Michael Smith Genome Sciences Centre, BC Cancer Agency, 570 W 7th Ave, Vancouver, BC V5Z 4S6 Canada.

[6]Department of Pathology & Laboratory Medicine, BC Cancer Agency, 675 10th Ave West, Vancouver, BC V5Z 1L3, Canada.

[7]Translational Ovarian Cancer Research Program, London Health Science Centre, 339 Windermere Road, London, ON N6A 5A5, Canada.

[8]Department of Medical Genetics, University of British Columbia, 4500 Oak St, Vancouver, BC V6H 3N1, Canada.

[*]These authors are co-first authors and contributed equally to this work.

[†]Corresponding and joint senior authors

Corresponding Authors:

Mark Carey, MD, FRCSC.
Division of Gynaecologic Oncology
6th Floor, DHCC, 2775 Laurel Street, Vancouver, BC V5Z 1M9, Canada.
Phone: 604-875-4268; Email: mark.carey@ubc.ca

Colin C. Collins, PhD,
Vancouver Prostate Centre,
2660 Oak Street, Vancouver, BC, V6H 3Z6, Canada.
Phone: 604-875-4111 (ext. 6736); Email: ccollins@prostatecentre.com

Supplementary Figures

List of Figures

Supplemental Figures

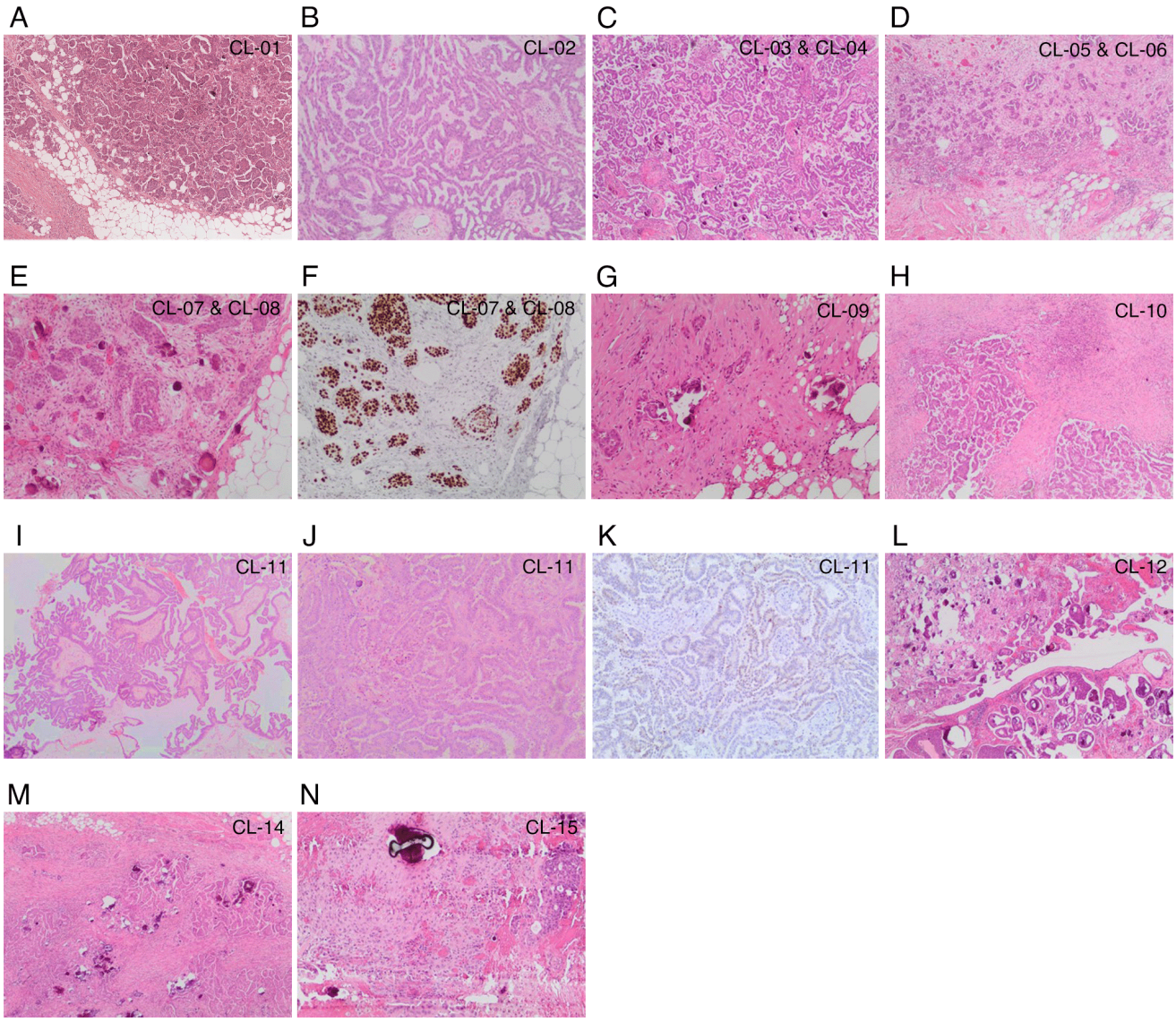

Supplementary Fig. S1. Histopathology of LGSOC. (A) Serous borderline tumor, micropapillary type CL-01 (iOV241Ca). (B) Serous borderline tumor micropapillary type CL-02 (VOA-1312). (C) Serous borderline tumor, micropapillary type CL-03 and CL-04 (VOA-1056 and VOA-3993). (D) LGSOC progressing from serous borderline tumor, micropapillary type CL-05 and CL-06 (VOA-3448 and VOA-3723). (E-F) LGSOC in a patient with germline BRCA1 inactivating mutation, displaying low-grade histology, (E) but a mutated pattern (over expression) of p53 staining by immunohistochemistry, (F) CL-07 and CL-08 (VOA-4627 and VOA-4698). (G) Low-grade serous carcinoma within involvement of omentum (without associated serous borderline tumor) CL-09 (VOA-6800). (H) Low-grade serous carcinoma arising from serous borderline tumor, micropapillary type CL-10 (VOA-6406). (I-K) Serous borderline tumor - micropapillary type (I) with associated LGSOC, (J) that display a wild-type pattern of p53 staining by immunohistochemistry, (K) CL-11 (VOA-6857). (L) LGSOC arising from serous borderline tumor, cribriform type CL-12 (VOA-7604). (M) LGSOC progressing from serous borderline tumor CL-14 (VOA-8862). (N) LGSOC arising from serous borderline tumor - micropapillary/cribriform type CL-15 (VOA-9164).

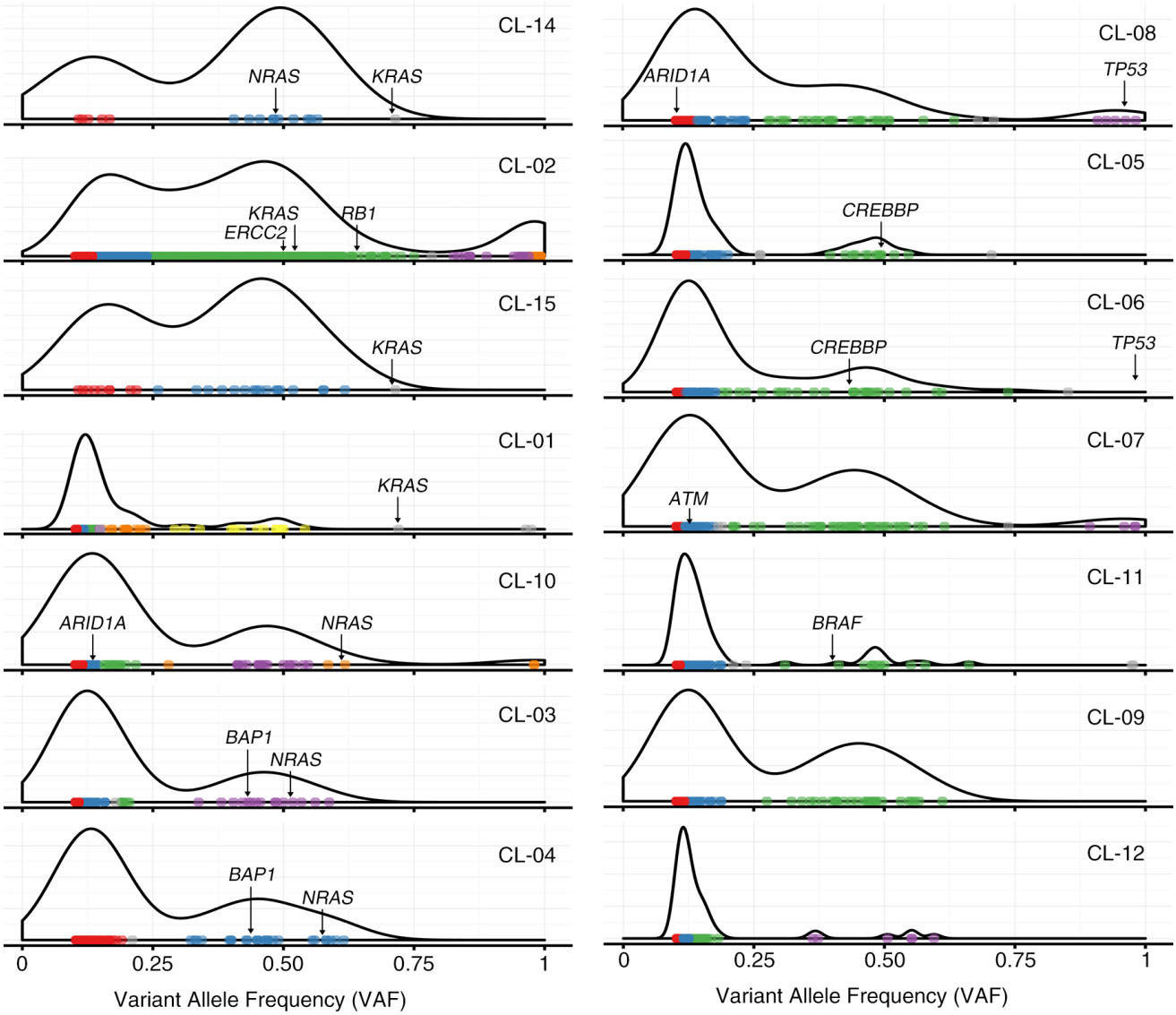

Supplementary Fig. S2. Distribution of variant allele frequency (VAF) of mutations in LGSOC. Based on VAF, the somatic mutations identified in LGSOC were clustered into different groups using the R-package Maftools. The horizontal axis represents the VAF of the mutations and the vertical axis represents its density.

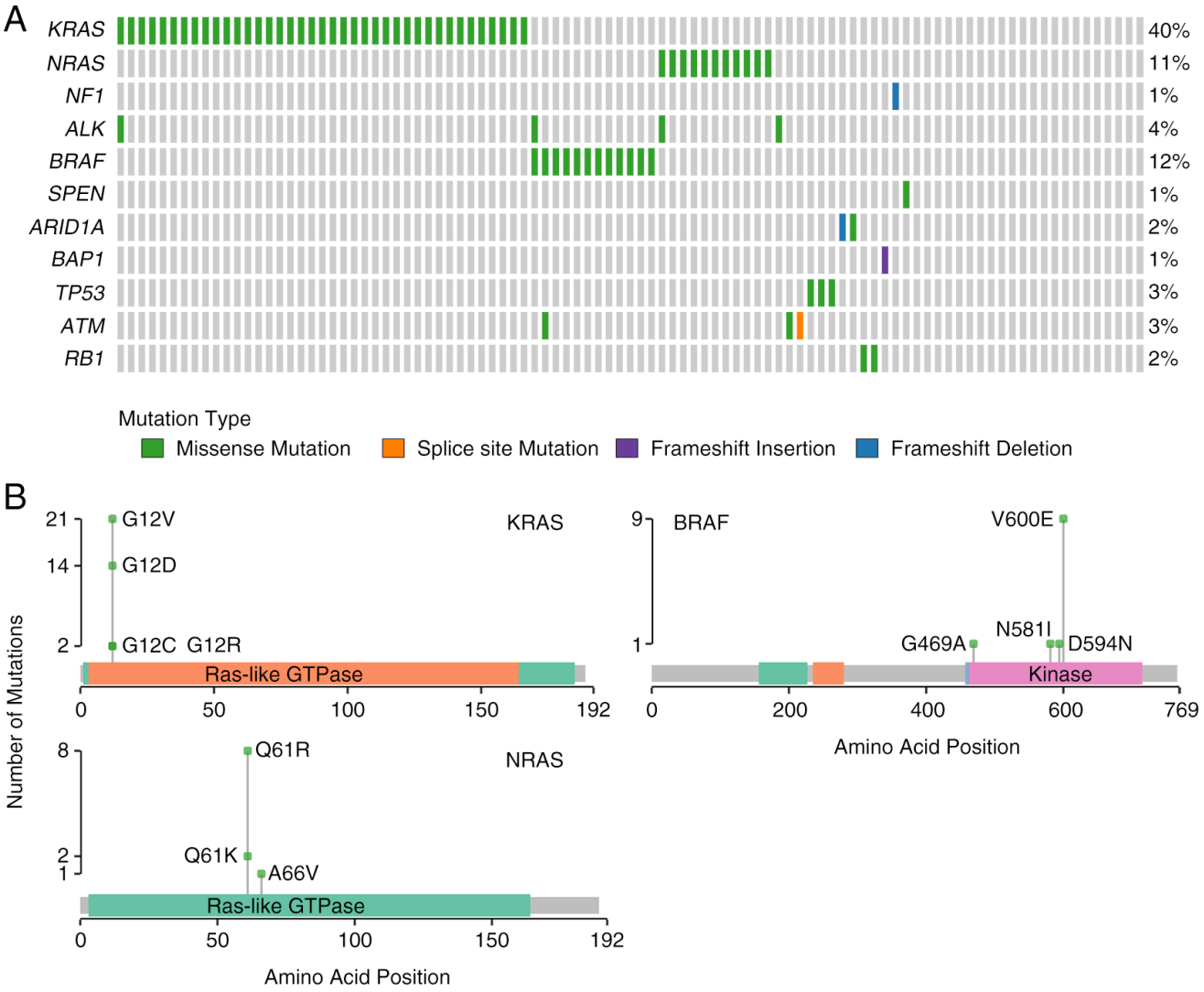

Supplementary Fig. S3. Somatic Mutation Landscape of LGSOC in AACR Project GENIE Cohort. (A) Oncoplot showing the status of mutated genes in major cancer pathways - MAPK pathway, Notch pathway, chromatin remodeling, and DNA repair pathway. Genes that overlap with those shown in Figure 1A is represented here. The numbers on the right of the plot shows the recurrence frequency (in percentage) of the corresponding mutation in the cohort. (B) Plots showing mutation distribution and the protein domains for the corresponding mutated protein.

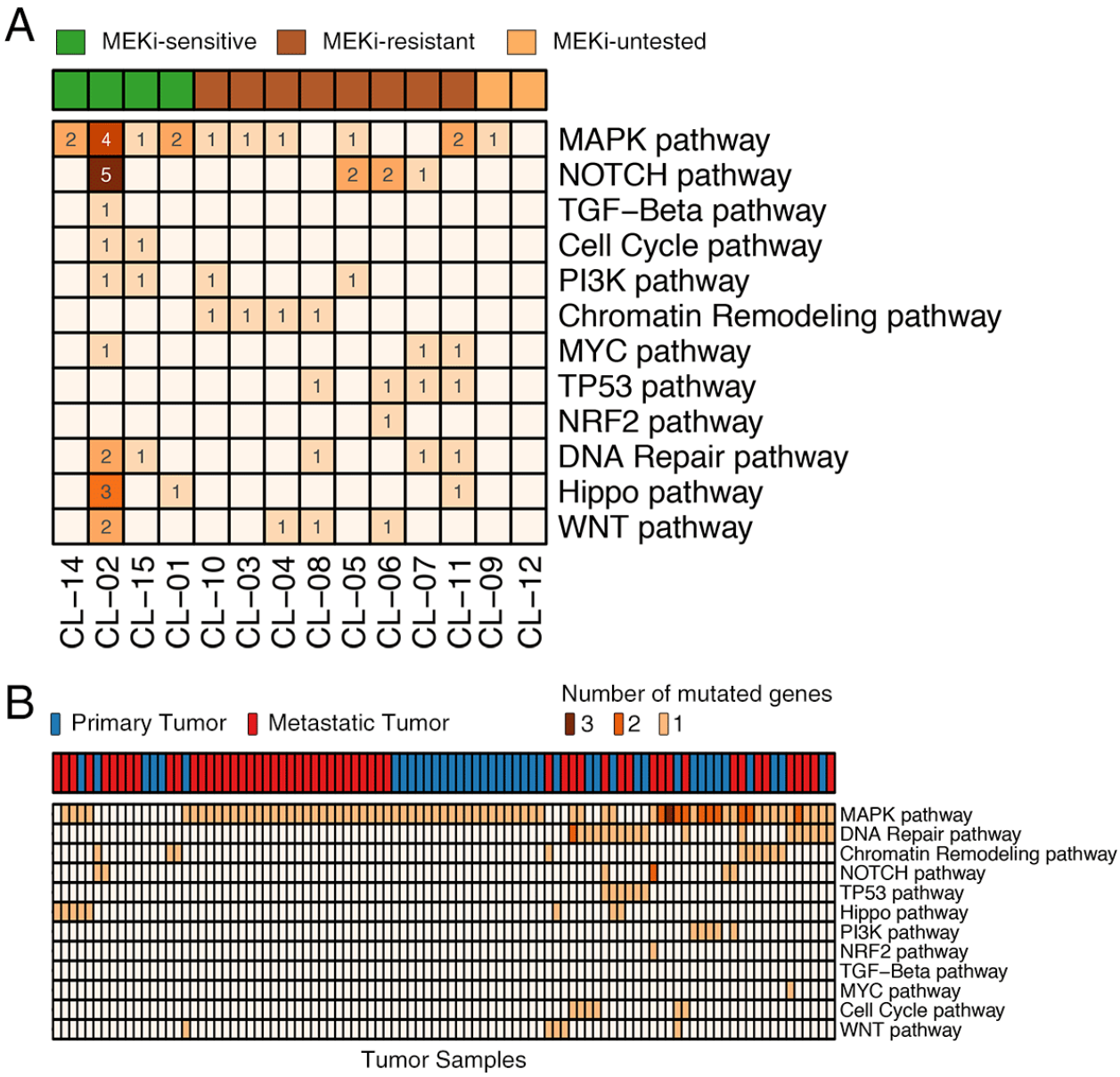

Supplementary Fig. S4. Mutated Oncogenic Pathways in LGSOC. (A) Heatmap showing the number of genes in the respective oncogenic pathways that are mutated per LGSOC cell line. The number of genes mutated in each pathway is indicated. (B) Mutated oncogenic pathways in LGSOC tumors from AACR Project GENIE. Heatmap showing the number of genes in the respective oncogenic pathways that are mutated per LGSOC tumor.

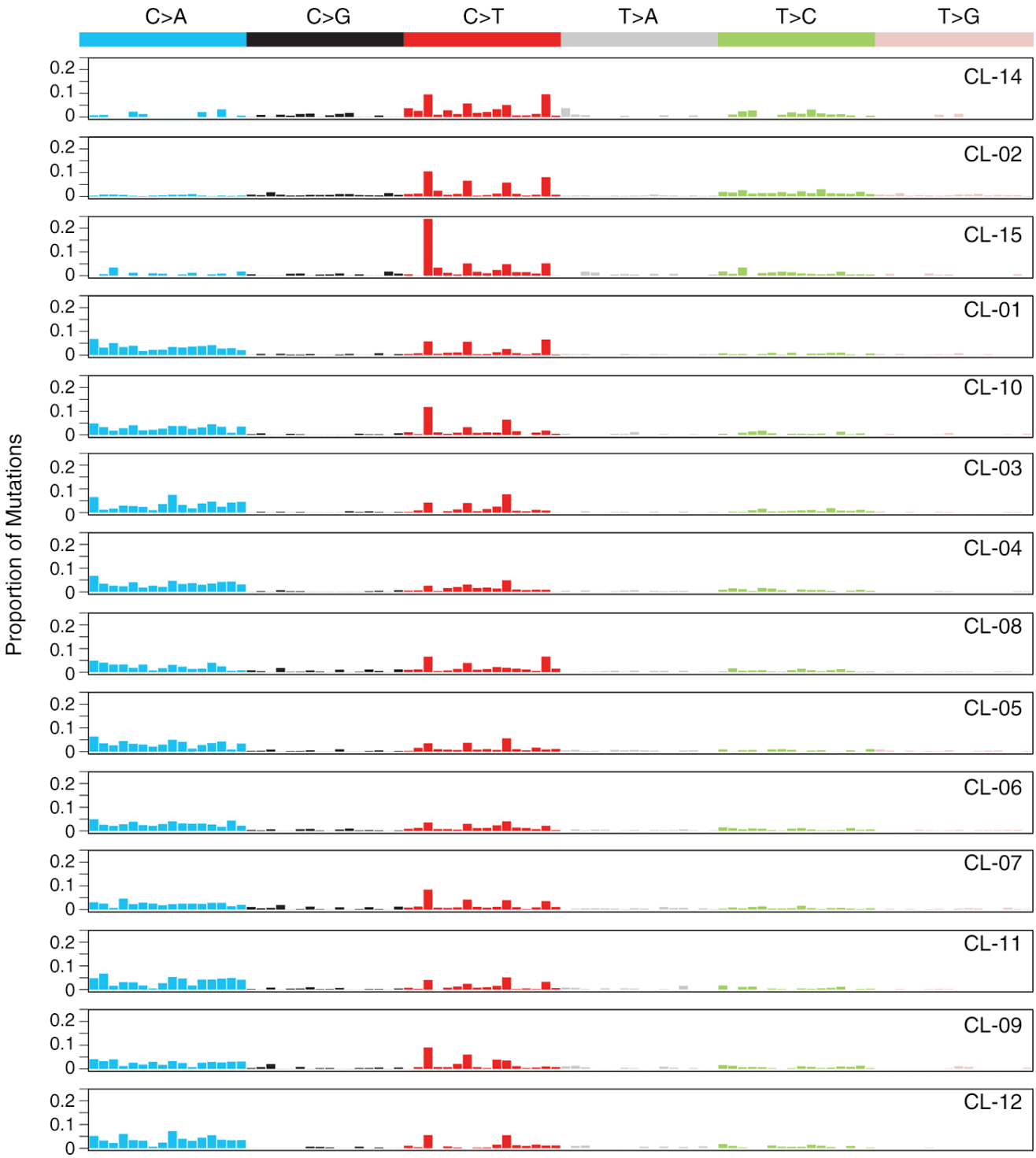

Supplementary Fig. S5. Nucleotide Substitution Mutation Patterns in LGSOC. The horizontal axis represents each of the 96 different possible combinations of the tri-nucleotide substitution mutation combinations colored by their respective substitution patterns. The vertical axis represents the proportion of mutations per sample.

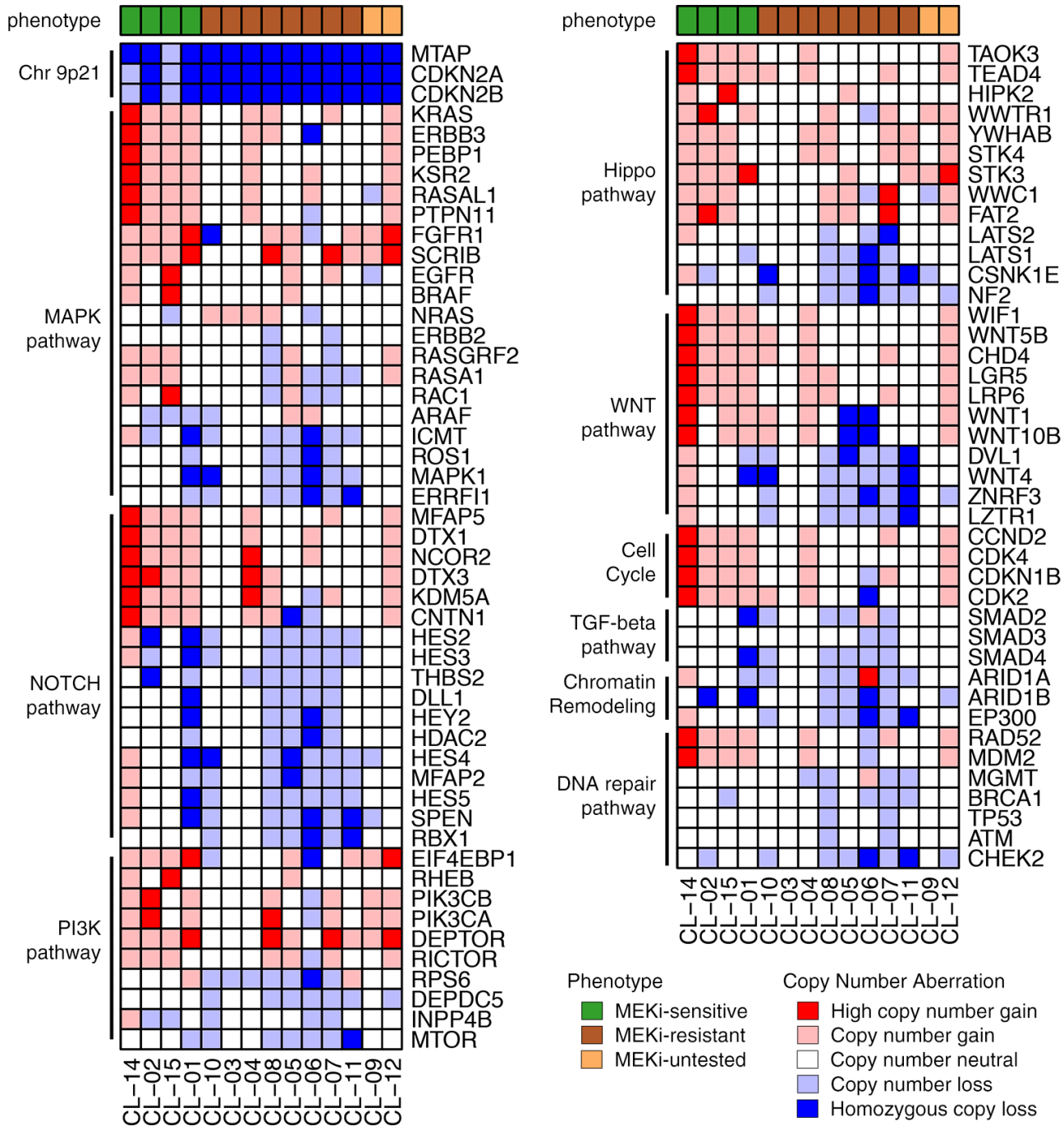

Supplementary Fig. S6. Copy number aberration status of LGSOC cell lines in oncogenic pathways. Heatmap showing the copy number status of genes grouped by different oncogenic pathways. In addition, genes in chromosome 9p21 are also shown.

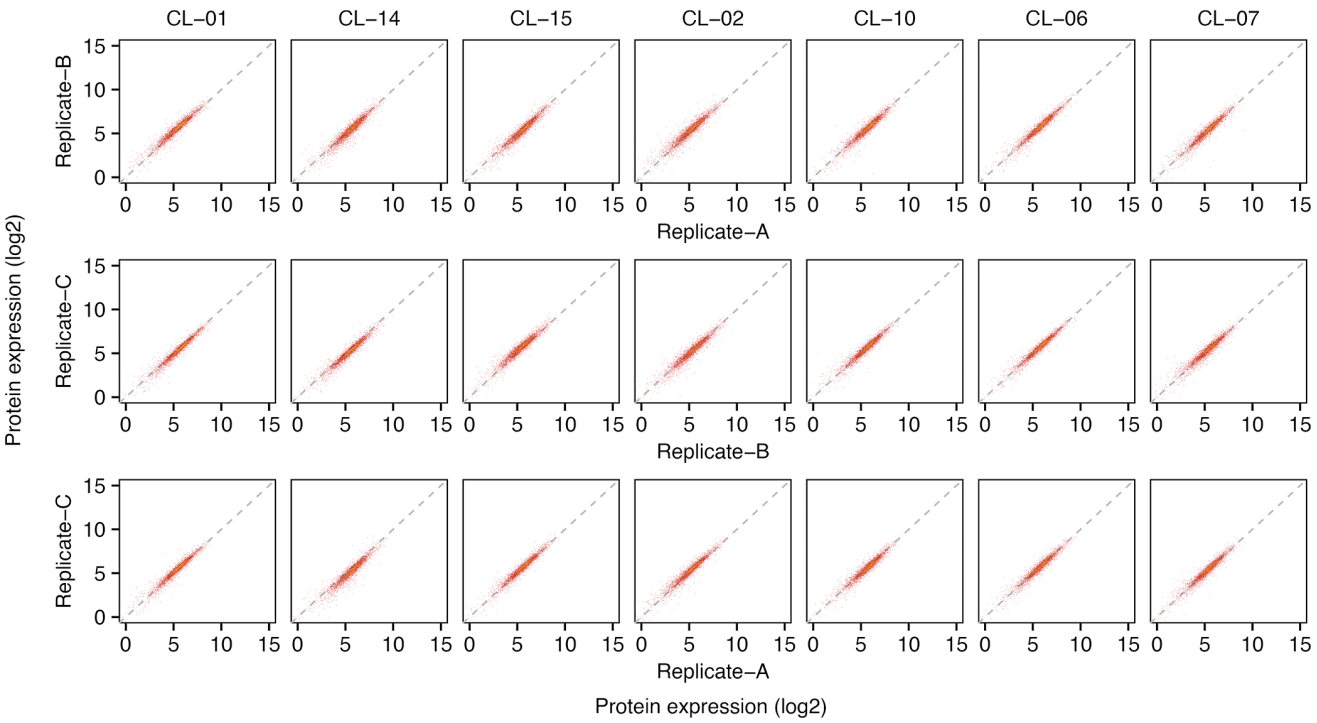

Supplementary Fig. S7. Protein expression correlation between the replicate sample pairs. The mass spectrometry proteome analysis on 7 LGSOC cell lines were profiled in triplicate. The above scatter plot compares the correlation of protein expression in the corresponding pair of replicates.

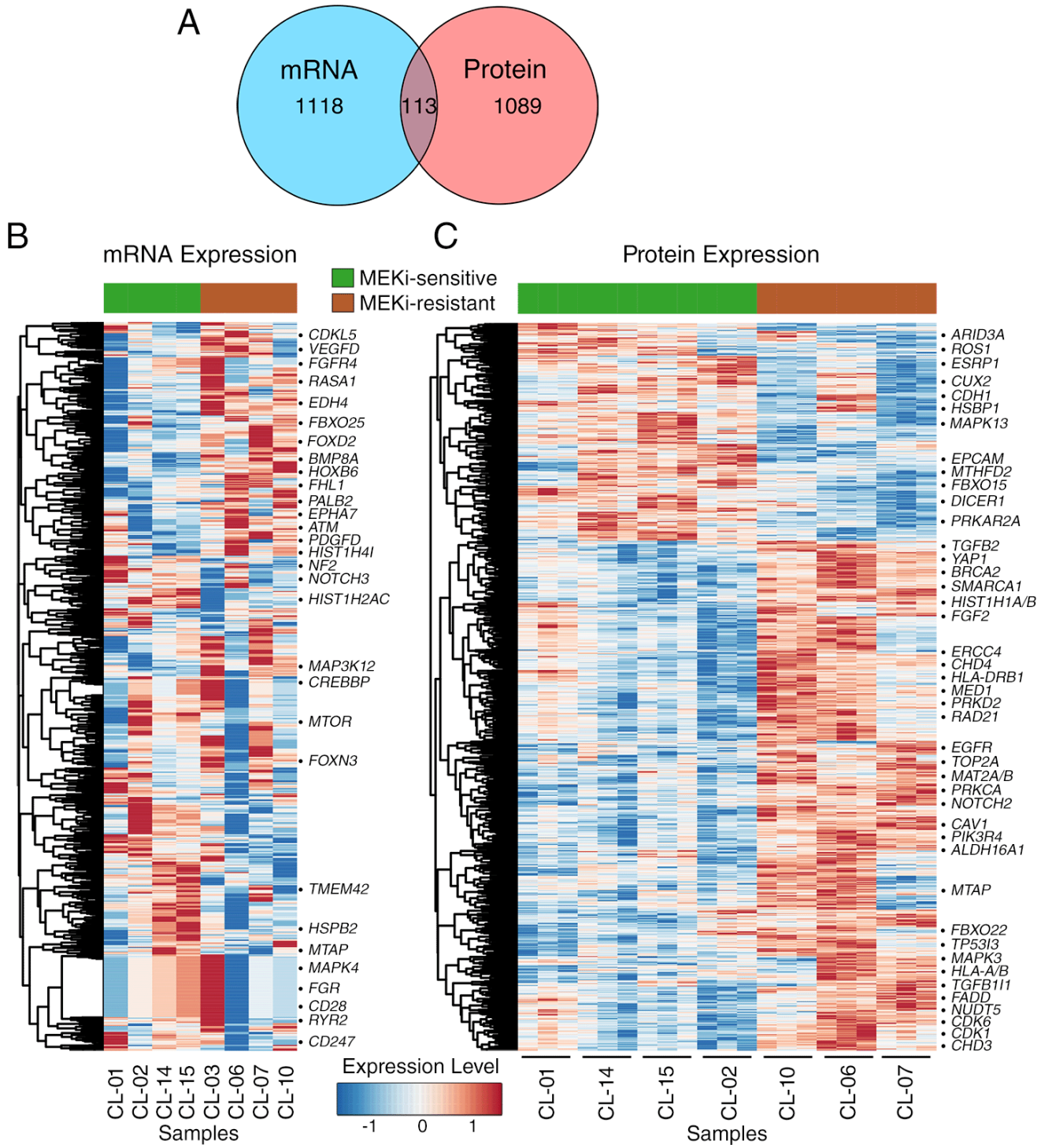

Supplementary Fig. S8. Significantly differentially expressed genes/proteins between the MEKi drug response phenotypes. (A) Venn diagram of overlap between the differentially expressed genes (from mRNA expression profiles) and proteins (from protein expression profiles) between the MEKi drug response phenotypes. (B-C) Heatmap of mRNA and protein expression profiles of the significantly differentially expressed genes/proteins between the MEKi- drug response phenotypes. The expression profile of each gene were mean normalized for visualization. Key differentially expressed genes have been highlighted.

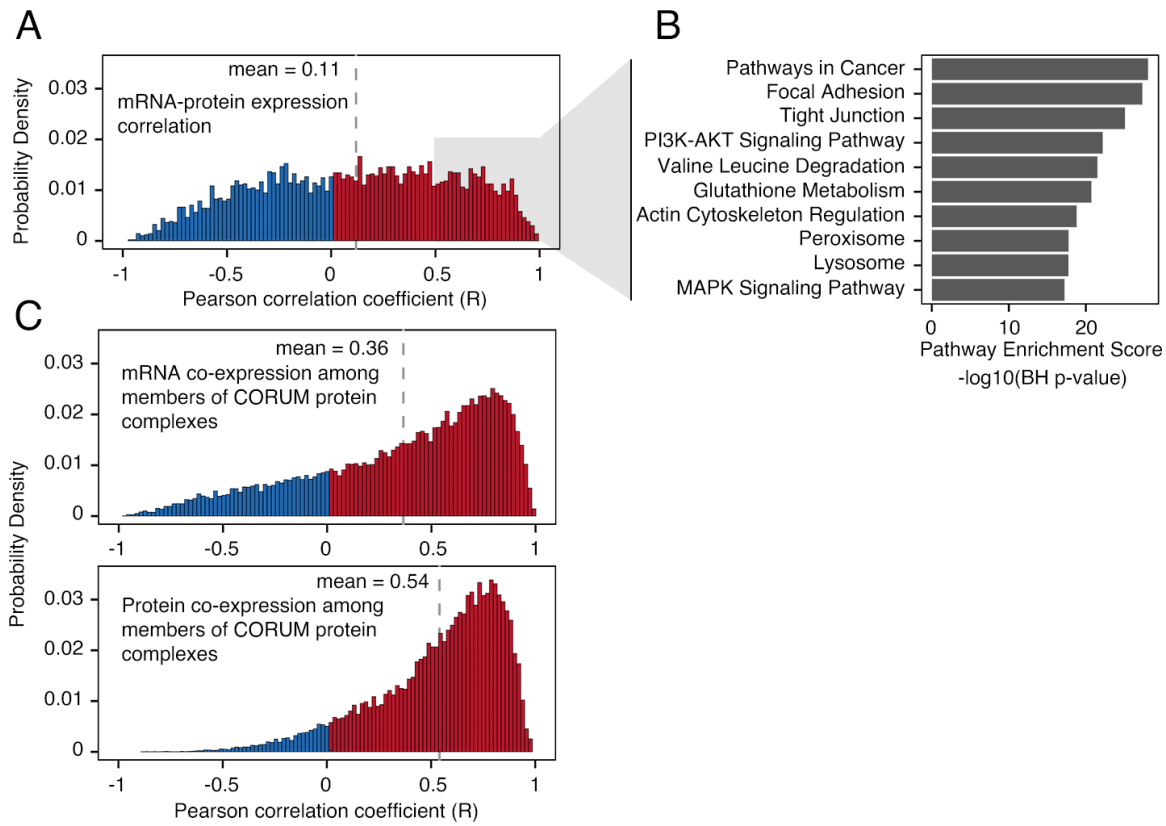

Supplementary Fig. S9. mRNA and protein correlation. (A) Histogram showing the distribution of Pearson correlation coefficient (R) of mRNA and protein expression correlation in LGSOC cell lines. Around 25% (1271 out of 4982) of proteins were highly correlated ($R \geq 0.5$) with their corresponding transcript abundance. (B) KEGG pathway enrichment of genes with high mRNA and protein expression correlation ($R \geq 0.5$). These highly correlated proteins were involved in different oncogenic signaling pathways including Focal adhesion, PI3-AKT pathway, and MAPK pathway. (C) Histogram showing the distribution of Pearson correlation coefficient (R) of mRNA co-expression and protein co-expression among the members of CORUM protein complexes. We compared the transcript abundances (co-expression) of a number of protein complex members. About 48% (24636 of 51275 gene pairs in 1701 protein complexes) of all gene pairs measured were highly correlated ($R \geq 0.5$). We also compared the protein abundances of these protein complex members. Interestingly, the protein abundance of protein complex members were highly co-expressed as compared to their respective transcripts. About 63% (22546 of 35411 protein pairs in 1008 protein complexes) of all protein pairs measured were highly correlated ($R \geq 0.5$).

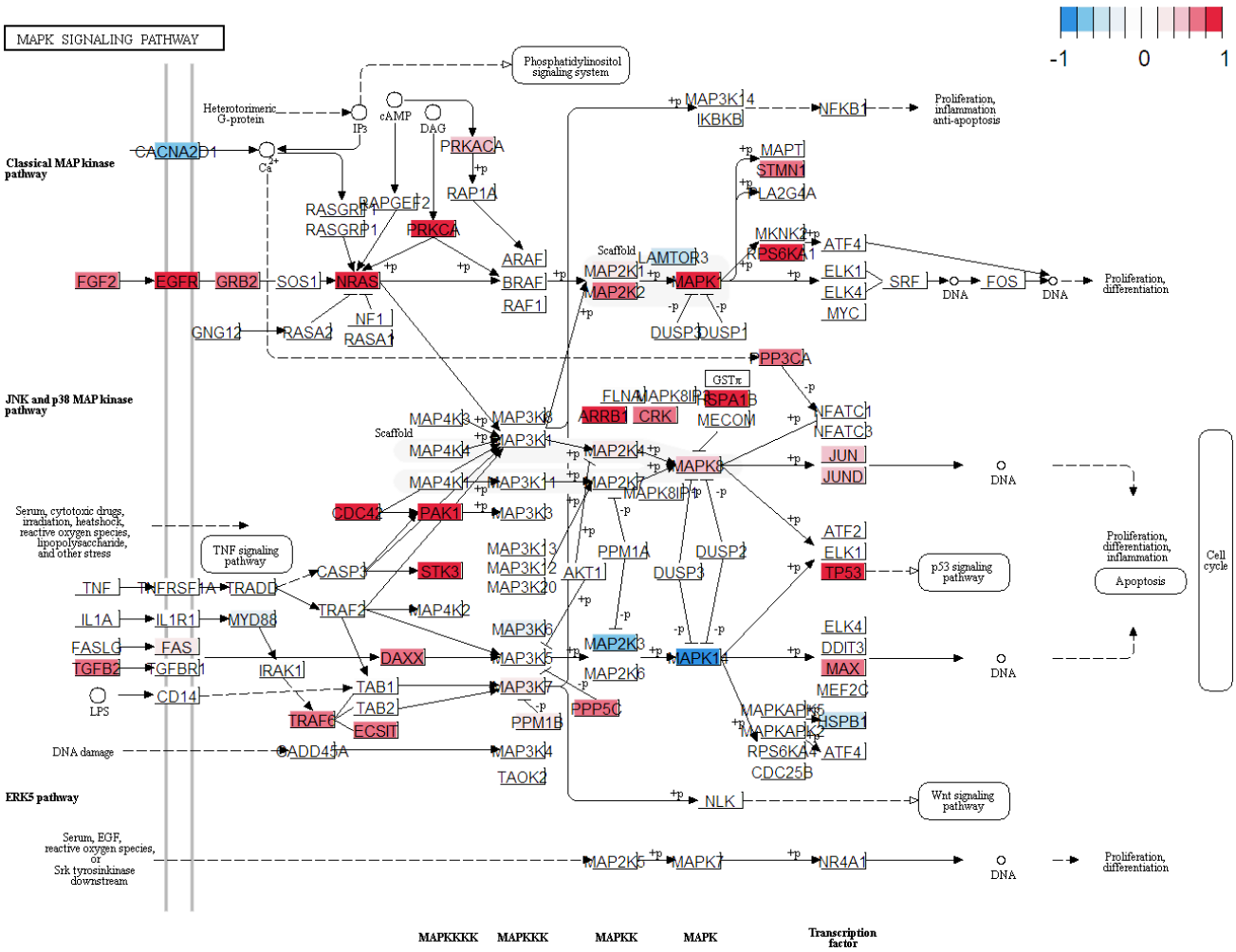

Supplementary Fig. S10. MAPK Signaling Pathway in MEKi-resistant LGSOC cell lines. Schematic overview of MAPK Signaling Pathway obtained from the KEGG pathway database. Individual proteins identified in the mass spectroscopy experiment were mapped into MAPK Signaling Pathway and their average protein expression profile in MEKi-resistant cell lines were visualized using *pathview* R-package.

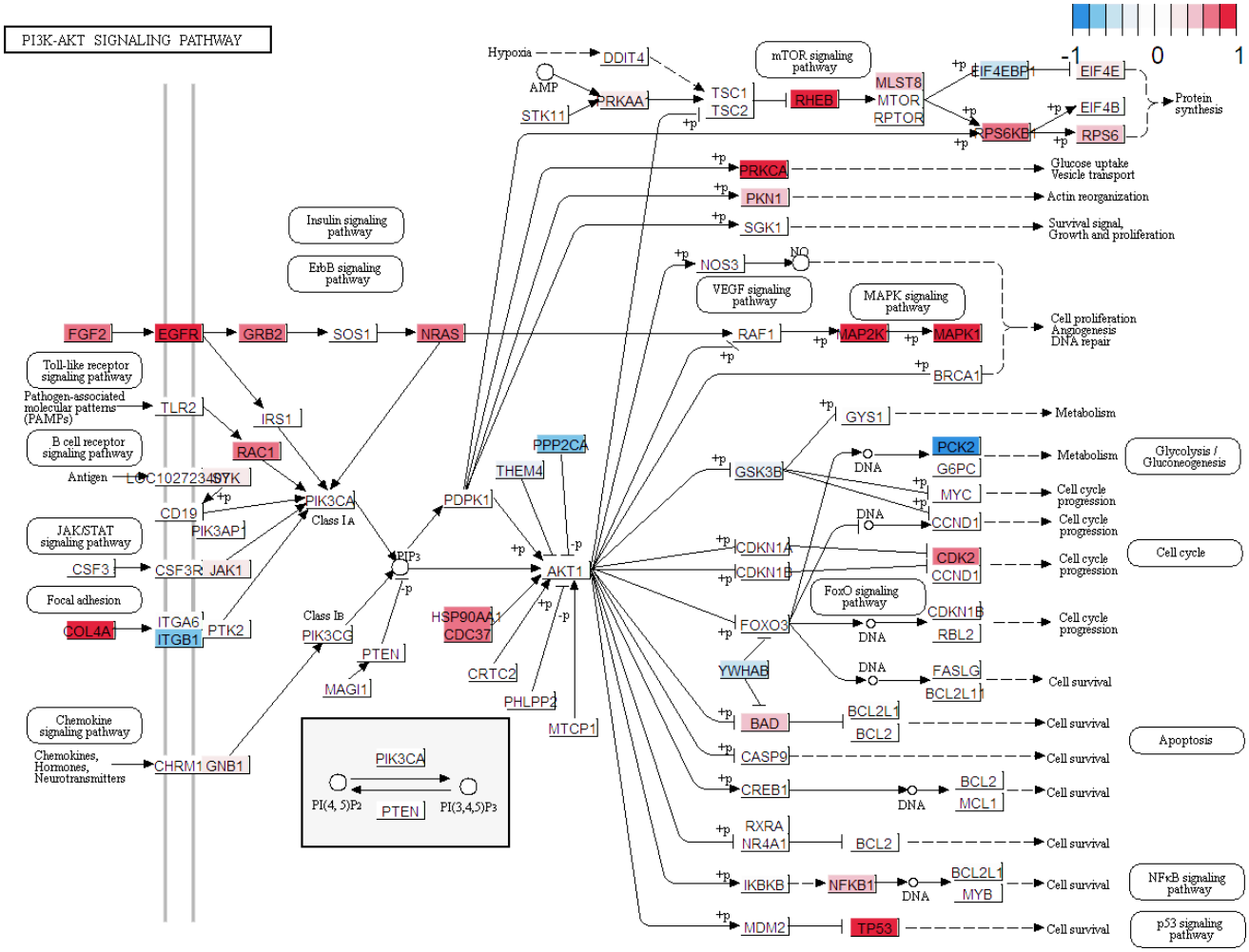

Supplementary Fig. S11. PI3K-AKT Signaling Pathway in MEKi-resistant LGSOC cell lines. Schematic overview of PI3K-AKT Signaling Pathway obtained from the KEGG pathway database. Individual proteins identified in the mass spectroscopy experiment were mapped into PI3K-AKT Signaling Pathway and their average protein expression profile in MEKi-resistant cell lines were visualized using *pathview* R-package.